# MODELING SIMULATION AND ANALYSIS OF TEXTILE PILLING BY USING UPGRADED PETRI NETS AND TWO-LEVEL EDGE DETECTION ALGORITHM

**Perica Štrbac[1], Miloš Pejanović[1], Mirjana Reljić[2]**

[1] Academy of Technical and Art Applied Studies,
School of Electrical and Computer Engineering, Belgrade
[2] CiS Institute, Vojislava Ilića 88, Belgrade
[*] e-mail: milos.pejanovicsp@viser.edu.rs

**Scientific paper**
UDC: 677-037:677-022: 62-4
DOI: 10.5937/tekstind2202012S

**Abstract:** *Upgraded Petri nets and a two-level edge detection algorithm for the modeling, simulation, detection, and analysis of textile pilling has used in this paper. There are two models in this paper. The first model is related to creating images with pilling on textiles. This model is represented at a low level of abstraction, using parallelism, synchronization, and preservation of model markup. After several iterations of the modeling, simulation, and analysis, the model transformed into a specific Python program. This program generates several hundred images of pilling on textiles. The second model refers to the modeling, simulation, and analysis of the preparation of generated images for entry into a program that uses a two-level algorithm for edge detection and generation of output images of detected pilling. An image preparation includes comparing pixel blocks (2x2, 4x4, and 8x8) of the image with textile pilling and the image without pilling. This image with pilling is modified regardless of the difference between the corresponding blocks. This image is an input to the two-level edge detection algorithm. The paper presents some examples of generated images of textile pilling and images with detected pilling. Errors due to the size of the comparison block about the exact pilling surface shown. The speed of image processing according to the size of the comparison blocks analyzed. Some guidelines represented for further research on pilling detection using Upgraded Petri nets and a two-level edge detection algorithm.*

**Keywords:** Upgraded Petri-nets, pilling, textile, algorithm, edge detection.

# MODELOVANJE SIMULACIJA I ANALIZA PILINGA POMOĆU NADGRAĐENIH PETRI MREŽA I DVONIVOVSKOG ALGORITMA ZA DETEKCIJU IVICA

**Apstrakt:** *U ovom radu korišćene su Nadgrađene Petri-mreže i dvonivovski algoritam za detekciju ivica za modelovanje, simulaciju, detekciju i analizu pilinga tekstila. Prikazana su dva modela. Prvi model se odnosi na kreiranje slika sa pilingom na tekstilu. Ovaj model je prikazan na niskom nivou apstrakcije, korišćenjem paralelizma, sinhronizacije i očuvanja markiranja modela. Nakon detaljne sekvence modelovanje – simulacija – analiza model je transformisan u konkretan Python program. Ovaj program je poslužio za generisanje nekoliko stotina slika pilinga na tekstilu. Drugi model se odnosi na modelovanje, simulaciju i analizu pripreme generisanih slika za ulaz u program koji koristi dvonivovski algoritam za detekciju ivica te generisanje izlaznih slika detektovanog pilinga. Priprema slika obuhvata poređenje blokova piksela 2x2, 4x4 te 8x8 slike sa pilingom tekstila sa osnovnom slikom bez pilinga. Na osnovu razlike pripadnih blokova modifikuje se slika pilinga koja će predstavljati ulaz u dvonivovski algoritam za detekciju ivica. U radu su prikazani primeri generisanih slika pilinga tekstila te slika sa detektovanim*

*pilingom. Prikazane su greške koje nastaju zbog veličine bloka za komparaciju u odnosu na ekgzaktnu površinu pilinga. Analizirana je brzina obrade slike prema veličini blokova poređenja. Date su smernice za dalja istraživanja detekcije pilinga korišćenjem Nadgrađenih Petri-mreža i dvonivovskog algoritma za detekciju ivica.*

**Ključne reči:** Nadgrađene Petri-mreže, piling, tekstil, algoritam, detekcija ivica.

## 1. INTRODUCTION

In the case of textile products made of fibers with a smooth surface, there is a tendency to form knots on the surface that is exposed to friction, i.e., a "pilling" effect appears [1]. The formation of the pilling effect is especially pronounced in fabrics and knitwear made of poly-amide fibers or a mixture of poly-amide and other fibers [2]. This disadvantage is especially pronounced in the exploitation of clothing due to friction [3].

Testing and control of textiles is performed in modern laboratories [4]. There are several tests to examine the effect of pilling. All tests use a sample of fabric that is exposed to friction in laboratory conditions. Samples are treated in several cycles (rotational and translational), where the values of the pilling test are determined on the basis of scale:

5 - no pilling;

4 - small pilling;

3 - moderate pilling;

2 - pronounced pilling;

1 - very pronounced pilling. [5]

The values of pilling are assessed by experts, visually in the laboratory, where human factors are present in determining the test results. The goal of testing is to achieve maximum objectivity and precision in determining test results [6].

This paper presents the results of modeling, simulation and analysis of image detection of textile samples on the example of determining the value for pilling, using specially designed software. The results of this work can be used to introduce fully automated processes in the textile industry, such as laboratory testing of textiles for water repellency (analysis of water droplets) or analysis and design of textile products using the concept of edge detection [7].

## 2. UPGRADED PETRI NETS

The Upgraded Petri-Net formal theory is based on functions and it is a nine-tuple [8]:

$C = (P, T, F, B, \mu, \theta, TF, TFL, PAF)$,

$P=\{p_1, p_2, p_3, ..., p_n\}$, $n>0$ *is a* finite nonempty set of places $p_i$. $T=\{t_1, t_2, t_3, ..., t_m\}$, $m>0$ *is a* finite nonempty set of transitions $t_j$.

$F:T\chi P\rightarrow N_0$ is an input function. $B:T\chi P\rightarrow N_0$ is an output function. $\mu:P\rightarrow N_0$ is a marking function.

$\theta:T\chi\Delta\rightarrow\lambda$ *is* a timing function. $TF:T\rightarrow$ A is a transition function. $TFL: T\rightarrow N_0$ is a transition firing level. $PAF: P\rightarrow (x, y)$ is a place attributes function. $N_0$ represents the set of non-negative integers.

For all details of the theory see [9].

## 3. TWO-LEVEL EDGE DETECTION ALGORITHM

Two-level edge detection algorithm is based on the Canny edge detection algorithm [10].

The first level includes loading a color image with three color planes and its transformation into a gray image with one (gray) plane.

We use contrast stretching of the gray image, and apply Gaussian blur on the newly obtained image. After that, we apply a double threshold over a blurred image.

The second level includes calculating the gradient according to the pixels of the image resulting from the first level, suppressing the non-maximum, retaining pixels of strong edges and retaining pixels of weak edges associated with the strong edge.

For all details of two-level edge detection algorithm see [11].

## 4. UPN MODELS

We show two UPN models. The first one refers to a model of creating images with pilling, while the second one refers to pilling detection. The Upgraded Petri-nets execution rules have been used in all models in the paper [1].

The first model is shown at figure 1. (the first part) and figure 2. (the second part). An initial marking of the UPN model is $\mu(p_1) = \mu(p_3) = \mu(p_4) = \mu(p_6) = \mu(p_7) = \mu(p_9) = \mu(p_{10}) = \mu(p_{11}) = \mu(p_{12}) = \mu(p_{14}) = \mu(p_{15}) = \mu(p_{16}) = \mu(p_{19}) = \mu(p_{20}) = \mu(p_{21}) = \mu(p_{22}) = \mu(p_{23}) = \mu(p_{24}) = \mu(p_{25}) = \mu(p_{26}) = \mu(p_{27}) = \mu(p_{28}) = \mu(p_{32}) = \mu(p_{33}) = \mu(p_{36}) = \mu(p_{37}) = \mu(p_{38}) = \mu(p_{39}) = \mu(p_{41}) = \mu(p_{42}) = \mu(p_{43}) = \mu(p_{44}) = 1$, and $\mu(p_{87}) = 5$. At this moment the transition $t_1$ (G_INIT) is enabled. By firing of this transition, the marking of the model changes ($\mu(p_1) = 0$, $\mu(p_2) =$

1), and it models start of graphical system initialization. Now, the transition $t_2$ (G_INIT_DISPLAY_MODE) is enabled. After firing of this transition, the marking of the model changes ($\mu(p_2) = 0$, $\mu(p_3) = 0$, $\mu(p_4) = 0$, $\mu(p_5) = 1$). The place $p_3$ (G_RGB) models RGB mode of a pixel presentation, while the place $p_4$ (G_DEPTH) models scene calculation with respect to depth of a pixel. After firing of the transition $t_2$, the transition $t_3$ (G_INIT_WINDOW_SIZE) is enabled. Input places of this transition are $p_6$ (G_WIDTH) and $p_7$ (G_HEIGHT), which x attributes are equal to 512. This means that the scene size is 512x512 pixels. After firing of the transition $t_3$, the marking of the model changes ($\mu(p_5) = \mu(p_6) = \mu(p_7) = 0$, $\mu(p_8) = 1$). At this moment, the transition $t_4$ (SET_CLEAR_COLOR) is enabled. By firing of this transition, the clear color is set as RGBA(1,0,0,1). These values are determined by values of x attributes places $p_9$ (CCR), $p_{10}$ (CCG), $p_{11}$ (CCB), and $p_{12}$ (CCA) respectively. The marking of the model changes ($\mu(p_8) = \mu(p_9) = \mu(p_{10}) = \mu(p_{11}) = \mu(p_{12}) = 0$, $\mu(p_{13}) = 1$). After firing of this transition, the transition $t_5$ (SET_COLOR) is enabled. By firing of the transition $t_5$, the color of the scene is determined by values of the x attributes of the places $p_{14}$ (CR), $p_{15}$ (CG), and $p_{16}$ (CB) respectively. The marking of the model changes ($\mu(p_{13}) = \mu(p_{14}) = \mu(p_{15}) = \mu(p_{16}) = 0$, $\mu(p_{17}) = 1$).

At this moment the transition $t_6$ (SET_SHADE_MODEL) is enabled. By firing of this transition, shade model of the scene is set as SMOOTH (modeled by place $p_{19}$) and the transition $t_7$ is enabled. The marking of the model changes ($\mu(p_{17}) = \mu(p_{19}) = 0$, $\mu(p_{18}) = 1$). By firing of the transition t7, in the scene will be enabled cull test, depth test and lighting. These features are determined by places $p_{20}$ (GL_CULL_FACE), $p_{21}$ (GL_DEPTH_TEST), and $p_{22}$ (GL_LIGHTING). After the firing, the marking of the model changes ($\mu(p_{18}) = \mu(p_{20}) = \mu(p_{21}) = \mu(p_{22}) = 0$, $\mu(p_{29}) = 1$). At this moment the transition $t_8$ (SET_L0_POS) is enabled. By firing of this transition position of the light 0 will be set according to values of the x attributes of the places $p_{23}$ (L0_POS_X), $p_{24}$ (L0_POS_Y), and $p_{25}$ (L0_POS_Z), i.e. (0, 0, -5).

After the firing, the marking of the model changes ($\mu(p_{29}) = \mu(p_{23}) = \mu(p_{24}) = \mu(p_{25}) = 0$, $\mu(p_{30}) = 1$). At this moment the transition $t_9$ (SET_L0_DIFF_L) is enabled. After firing of the transition $t_9$, new value of diffuse component of the light 0 will be set as (0.5, 0.5, 0.5) with respect to values of the attributes x of the places $p_{26}$ (L0_DIFF_COLL_R), $p_{27}$ (L0_DIFF_COLL_G), and $p_{28}$ (L0_DIFF_COLL_B). Now, the marking of the model changes ($\mu(p_{26}) = \mu(p_{27}) = \mu(p_{28}) = \mu(p_{30}) = 0$, $\mu(p_{31}) = 1$), and the transition $t_{10}$ (SET_L0_ATTENUATION) is enabled. By firing of the transition $t_{10}$ the attenuation properties of the light 0 will set as the follows: constant attenuation at values 0.1, and linear attenuation at 0.05. These values are determined by values of the x attributes of the places $p_{32}$ (GL_CONSTANT_ATTENUATION), and $p_{33}$ (GL_LINEAR_ATTENUATION). Now, the marking of the model changes ($\mu(p_{31}) = \mu(p_{32}) = \mu(p_{33}) = 0$, $\mu(p_{34}) = 1$), and the transition $t_{11}$ (GL_ENABLE_L0) is enabled. By firing of the transition $t_{11}$ (GL_ENABLE_L0) will enable light 0, and the model marking changes ($\mu(p_{34}) = 0$, $\mu(p_{35}) = 1$). Also, the transition $t_{12}$ (SET_ORTHO_2D_PROJ) is enabled. After firing of this transition orthogonal projection of the scene will set. Setting values are: left x = -1, right x = 1, bottom y = -1, top y = 1 and it is determined by values of the x attributes of the places $p_{36}$ (ORTHO2D_LX), $p_{37}$ (ORTHO2D_RX), $p_{38}$ (ORTHO2D_DY), $p_{39}$ (ORTHO2D_UY), respectively.

After the firing, the marking of the model changes ($\mu(p_{35}) = \mu(p_{36}) = \mu(p_{37}) = \mu(p_{38}) = \mu(p_{39}) = 0$, $\mu(p_{40}) = 1$). Now, the transition $t_{13}$ (SET_VIEW_PORT) is enabled. By firing of this transition will be set view port of the scene regarding to x values of the transitions $p_{41}$ (WP_DLX), $p_{42}$ (WP_DLY), $p_{43}$ (WP_WIDTH), and $p_{44}$ (WP_HEIGHT). View port coordinates are 0, 0, 512, 512. After the firing, the marking of the model changes ($\mu(p_{40}) = \mu(p_{41}) = \mu(p_{42}) = \mu(p_{43}) = \mu(p_{44}) = 0$, $\mu(p_{45}) = 1$). Now, the transition $t_{14}$ (SET_MATRIX_MODE) is enabled. By firing of the transition t14 will be set model view matrix mode (according to the place p46 (GL_MODEL_VIEW)). The place $p_{46}$ has inhibitor output arc. After the firing, the marking of the model changes ($\mu(p_{45}) = 0$, $\mu(p_{47}) = 2$). Back function $B(t_{14}, p_{47}) = 2$, so there are two output arcs. At this moment the set of transitions $\{t_{15}, t_{16}\}$ is enabled for parallel firing of these transitions. Parallel firing of the transitions $t_{15}$ (CLEAR_DEPTH), and $t_{16}$ (CLEAR_COLOR) will clear depth buffer, and color buffer. The marking of the model changes ($\mu(p_{47}) = 0$, $\mu(p_{48}) = 1$). Front function $F(t_{17}, p_{48}) = 2$ so there are two input arcs. There is an inhibit arc between place $p_{49}$ (TEXTURE), and transition $t_{17}$. At this moment the transition $t_{17}$ (READ_TEXTURE) is enabled. By firing of this transition will load texture determined by place $p_{49}$. After the firing, the marking of the model changes ($\mu(p_{48}) = 0$, $\mu(p_{50}) = \mu(p_{53}) = 1$). Now, the transition $t_{18}$ (ENABLE_TEXTURE) is enabled.

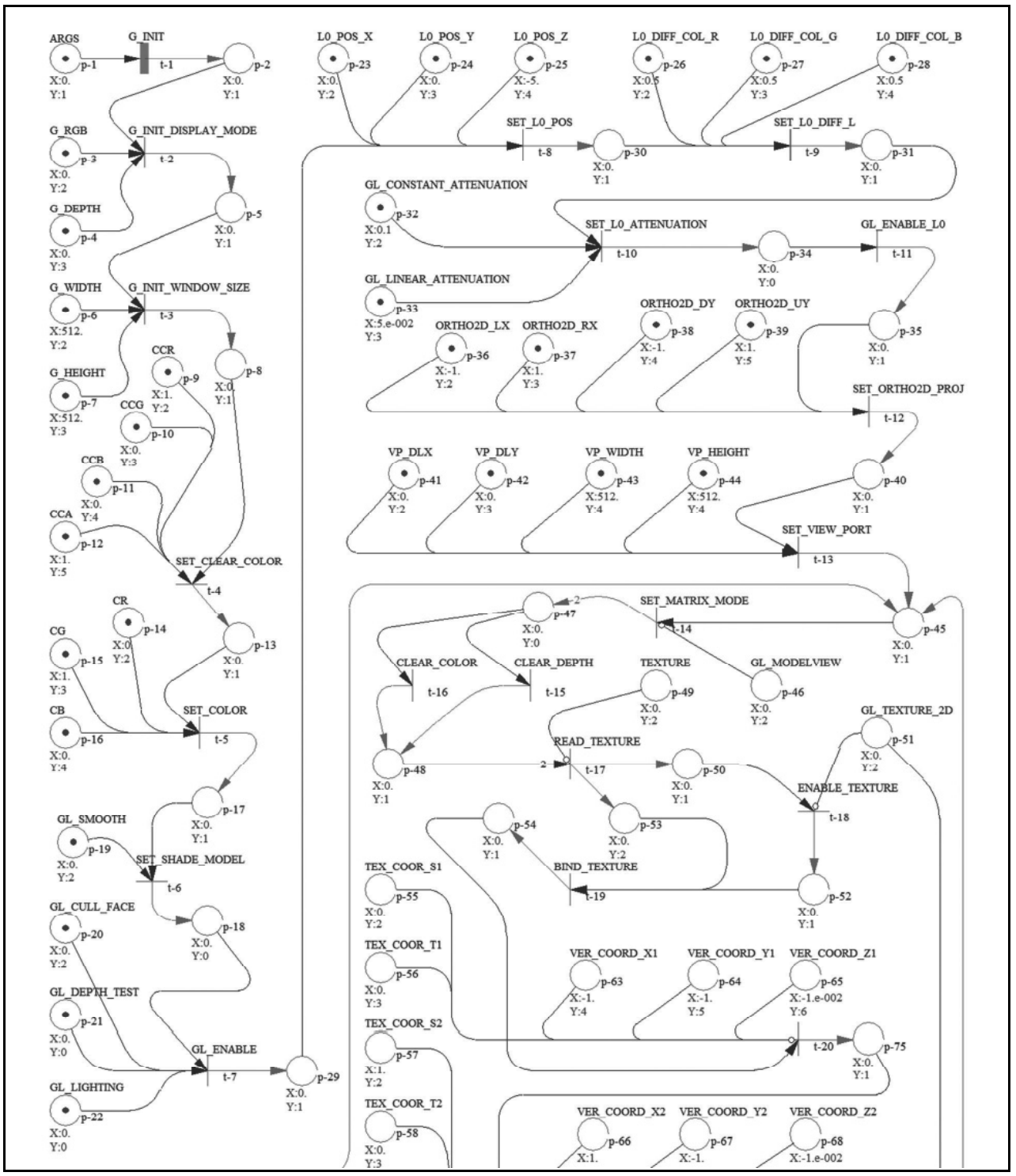


**Figure 1**: The UPN model of pilling, the first part

By firing of transition t18 will enable texture as 2D mapping textures (determined by place p51 (GL_TEXTURE_2D) with inhibitor output arc). The marking of the model changes (($\mu(p_{50}) = 0$, $\mu(p_{52}) = 1$)). At this moment the transition $t_{19}$ (BIND_TEXTURE) is enabled. After firing of this transition, the texture is chosen to use. Now, the marking of the model changes ($\mu(p_{52}) = 0$, $\mu(p_{54}) = 1$). At this moment the transition $t_{20}$ is enabled. By firing of this transition texture coordinates determined by values of x attributes of the places $p_{55}$ (TEX_COOR_S1), and $p_{56}$ (TEX_COOR_T1) will applied to the point determined by values of x attributes of the places $p_{63}$ (VER_COORD_X1), $p_{64}$ (VER_COORD_Y1), and $p_{65}$ (VER_COORD_Z1). The places $p_{55}$, $p_{56}$, $p_{63}$, $p_{64}$, and $p_{65}$ have input inhibitor to the place $t_{20}$. The marking of the model changes (($\mu(p_{54}) = 0$, $\mu(p_{75}) = 1$)). At this moment the transition $t_{21}$ is enabled.

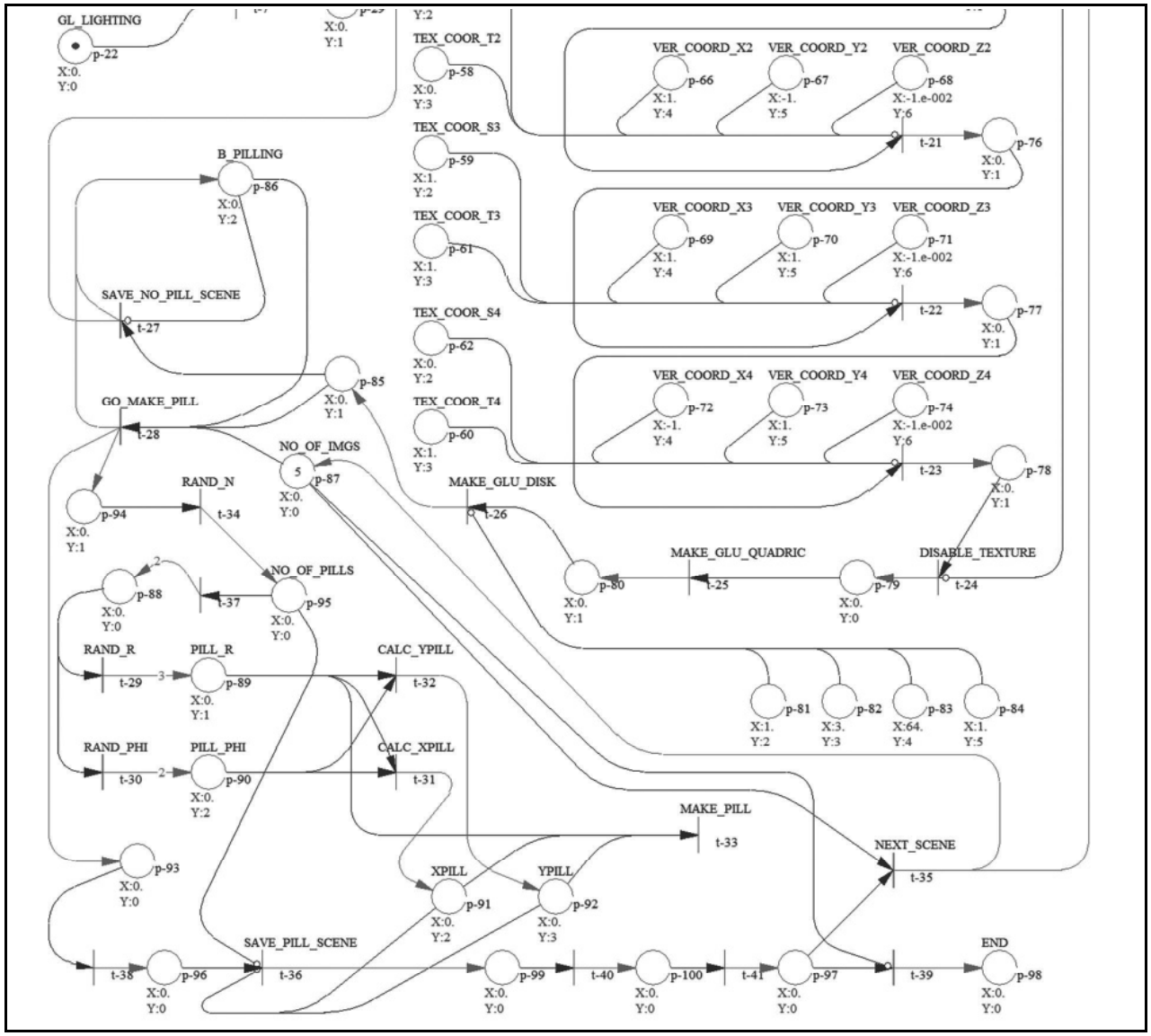


**Figure 2:** The UPN model of pilling, the second part

By firing of the transition $t_{21}$ texture coordinates determined by values of x attributes of the places $p_{57}$ (TEX_COOR_S2), and $p_{58}$ (TEX_COOR_T2) will applied to the point determined by values of x attributes of the places $p_{66}$ (VER_COORD_X2), $p_{67}$ (VER_COORD_Y2), and $p_{68}$ (VER_COORD_Z2). The places $p_{57}$, $p_{58}$, $p_{66}$, $p_{67}$, and $p_{68}$ have input inhibitor to the place $t_{21}$. The marking of the model changes (($\mu(p_{75}) = 0$, $\mu(p_{76}) = 1$)). At this moment the transition $t_{22}$ is enabled. By firing of the transition $t_{22}$ texture coordinates determined by values of x attributes of the places $p_{59}$ (TEX_COOR_S3), and $p_{61}$ (TEX_COOR_T3) will applied to the point determined by values of x attributes of the places $p_{69}$ (VER_COORD_X3), $p_{70}$ (VER_COORD_Y3), and $p_{71}$ (VER_COORD_Z3). The places $p_{59}$, $p_{61}$, $p_{69}$, $p_{70}$, and $p_{71}$ have input inhibitor to the place $t_{23}$. The marking of the model changes (($\mu(p_{77}) = 0$, $\mu(p_{78}) = 1$)). At this moment the transition $t_{23}$ is enabled. By firing of the transition $t_{23}$ texture coordinates determined by values of x attributes of the places $p_{62}$ (TEX_COOR_S4), and $p_{60}$ (TEX_COOR_T4) will applied to the point determined by values of x attributes of the places $p_{72}$ (VER_COORD_X4), $p_{73}$ (VER_COORD_Y4), and $p_{74}$ (VER_COORD_Z4). The places $p_{62}$, $p_{60}$, $p_{72}$, $p_{73}$, and $p_{74}$ have input inhibitor to the place $t_{23}$. The marking of the model changes (($\mu(p_{77}) = 0$, $\mu(p_{78}) = 1$)). At this moment the transition $t_{24}$ is enabled.

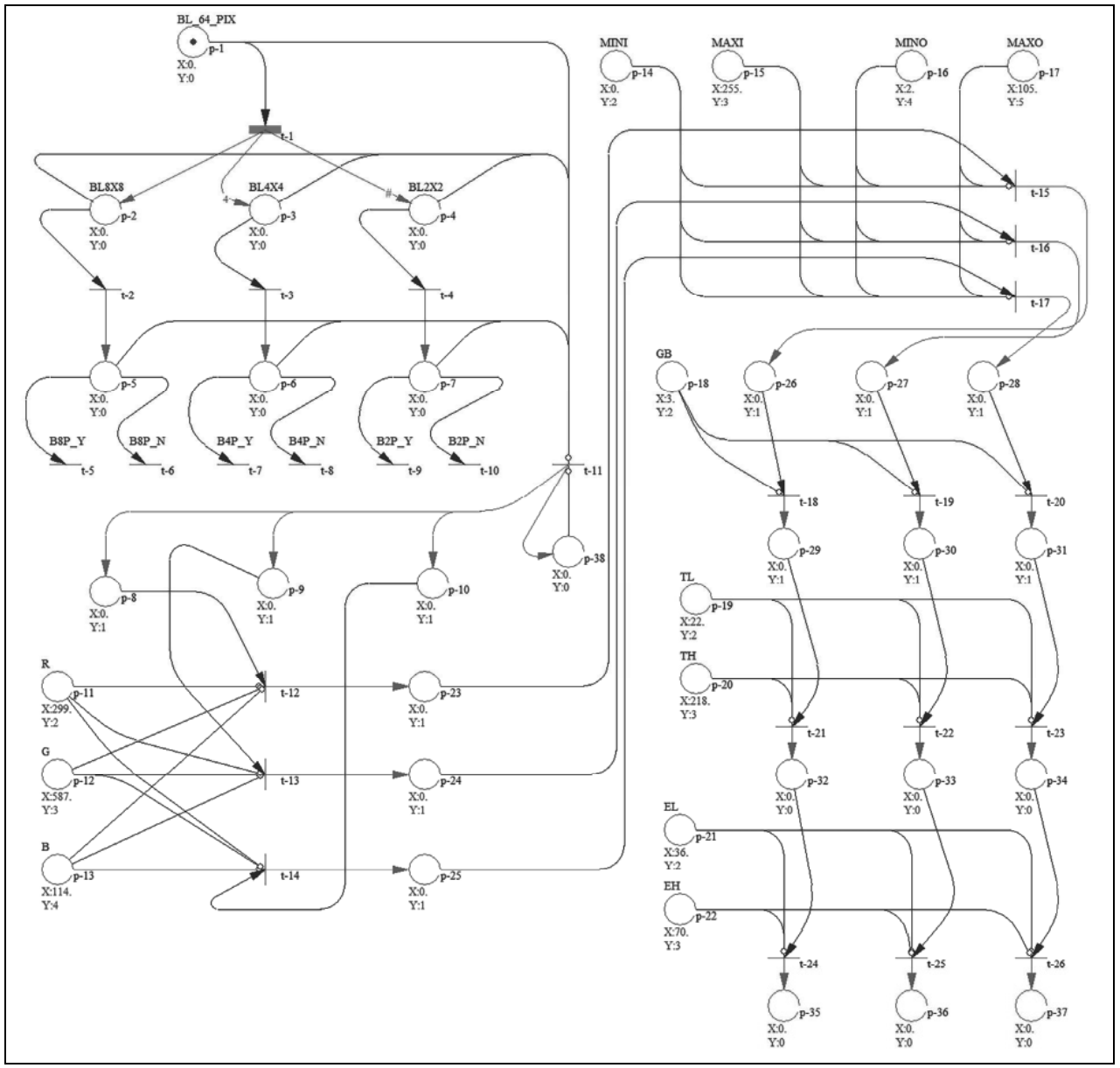


**Figure 3:** The UPN model of pilling detection

The sequence of firing transitions $\{t_{22}\}$, $\{t_{21}\}$, $\{t_{22}\}$, and $\{t_{23}\}$ refers to making rectangle in the scene with the texture. The next sequence of firing transitions $\{t_{24}\}$, $\{t_{25}\}$, $\{t_{26}\}$ make white disk with parameters $p_{81}$.x, $p_{82}$.x, $p_{83}$.x, and $p_{84}$.x. These parameters are inner r, outer r, slice, and loops, respectively. This disk is made by using a quadrics object. The sequence makes the marking of the model changes as follows (($\mu(p_{78}) = 0$, $\mu(p_{79}) = 1$)), (($\mu(p_{79}) = 0$, $\mu(p_{80}) = 1$)), and (($\mu(p_{80}) = 0$, $\mu(p_{85}) = 1$)). Now, the transition $t_{27}$ is enabled. This transition refers to saving no pilling scene. By firing of the transition $t_{27}$ the model returns to the point of making scene. We have again the sequence $\{t_{14}\}$, $\{t_{15}, t_{16}\}$, $\{t_{17}\}$, $\{t_{18}\}$, $\{t_{19}\}$, $\{t_{20}\}$, $\{t_{21}\}$, $\{t_{22}\}$, $\{t_{23}\}$, $\{t_{24}\}$, $\{t_{25}\}$, $\{t_{26}\}$. But now instead of $\{t_{27}\}$ it will be $\{t_{28}\}$ (GO_MAKE_PILL) because of $\mu(p_{86}) = 1$. By firing of the transition $t_{28}$ $\mu(p_{85}) = 1$ (save its marking), $\mu(p_{93}) = \mu(p_{94}) = 1$, and $\mu(p_{87}) = 4$. The marking of the place $p_{87}$ refers to number of pilling images we want to create (initially set to 5). Now, the set $\{t_{34}, t_{38}\}$ is enabled. The firing of the transition $t_{34}$ (RAND_N) will make marking of model changes ($\mu(p_{94}) = 0$, $\mu(p_{96}) = 1$, and $\mu(p_{95})$ will be set to a random number. The marking of the place $p_{95}$ (NO_OF_PILLS) refers to number of pillings that will be make in the scene. For example, let $\mu(p_{95}) = 3$. The firing of the transition $t_{38}$ will make marking of model changes $\mu(p_{93}) = 0$, $\mu(p_{96}) = 1$. At this moment the transition $t_{37}$ is enabled. After firing of this transition marking of model changes $\mu(p_{95}) = 2$, $\mu(p_{88}) = 2$. The sequence $\{t_{37}\}$, $\{t_{29}, t_{30}\}$, $\{t_{32}, t_{31}\}$, and $\{t_{33}\}$ three times occurs. This sequence will make 3 pilling at the scene. All 3 pills are random placed in circle with radius r and angle j. Radius r is

less than inner radius of disk. Now, $\mu(p_{95}) = 0$, so the transition $t_{36}$ is enabled. By firing of the transition, a new image with pilling will be saved, $\mu(p_{96}) = 0$, $\mu(p_{99}) = 1$, and $t_{40}$ is enabled. The sequence $\{t_{40}\}$, $\{t_{41}\}$ occurs. The transitions $t_{40}$ and $t_{41}$ are used for synchronization with sequence $\{t_{37}\}$, $\{t_{29}, t_{30}\}$, $\{t_{32}, t_{31}\}$, and $\{t_{33}\}$. If $\mu(p_{97}) = 1$ then only one of the two transitions, $t_{39}$ or $t_{35}$ will be enabled. If $\mu(p_{87}) = 0$ the transition $t_{39}$ is enabled.

After firing of the transition $t_{39}$, $\mu(p_{98}) = 1$, and it means that the model is reached death node. On the other side, if $\mu(p_{87}) > 0$ the transition $t_{35}$ is enabled. Front and back functions $F(t_{35}, p_{87}) = B(t_{35}, p_{87}) = 1$, and it preserve marking of the place $p_{87}$. After the firing of the transition $t_{35}$, the model goes to another cycle of making new pilling scene. This sequence repeats until $\mu(p_{87}) > 0$, and $\mu(p_{98}) = 0$.

The UPN model of pilling detection is shown at figure 3. The initial marking of the model is $\mu(p_1) = 1$. The place $p_1$ (BL_64_PIX) refers to picture has 64 pixels. The transition $t_1$ is enabled. By firing of this transition will change the marking of the model ($\mu(p_2) = 1$, $\mu(p_3) = 4$, $\mu(p_4) = 16$, $\mu(p_1) = 0$).

The place $p_2$ (BL8X8), $p_3$ (BL4X4) and $p_4$ (BL2x2) refer to block 8x8 pixels size, 4x4 pixels size, and 2x2 pixels size, respectively. Now, the set of transitions $\{t_2, t_3, t_4\}$ is enabled.

By firing of the set, the marking of the model changes ($\mu(p_2) = 0$, $\mu(p_3) = 3$, $\mu(p_4) = 15$, $\mu(p_5) = \mu(p_6) = \mu(p_7) = 1$). There are 3 conflicts ($p_5$, $t_5$, $t_6$), ($p_6$, $t_7$, $t_8$), ($p_7$, $t_9$, $t_{10}$). Anyone of them simulates a comparison between a block of an image with pilling and an appropriate image without pilling.

The blocks may be similar or not. In both case the image with pilling will be updated respect to the block.

When all markers from the places $p_2$, $p_3$ and $p_4$ is consumed the transition $t_{11}$ will be enabled.

By firing of this transition, the marking of the model changes ($\mu(p_8) = \mu(p_9) = \mu(p_{10}) = \mu(p_{38}) = 1$).

The marking $\mu(p_{38}) = 1$ will make the transition permanently disabled. The places $p_8$, $p_9$ and $p_{10}$ refer to updated image with pilling respect to comparable block size.

These images are inputs to the two-level edge detection algorithm (TLEDA).

The places denoted as R, G, B make a gray image of the input image. R.x, G.x and B.x determine ponder coefficients (x values: 299, 587, 114). By firing of the set $\{t_{12}, t_{13}, t_{14}\}$ program goes to the next stage of the TLEDA.

Now, the MINI.x, MAXI.x, MINO.x and MAXO.x determine contrast stretching parameters (x values: 0, 255, 2, 105). By firing of the set $\{t_{15}, t_{16}, t_{17}\}$ program goes to the next stage of the TLEDA.

At this moment, GB.x determine Gaussian blur (x value: 3). By firing of the set $\{t_{18}, t_{19}, t_{20}\}$ program goes to the next stage of the TLEDA. At this moment, TL.x and TH determine threshold low pixels and high pixels parameters, respectively (x values: 22, 218). By firing of the set $\{t_{21}, t_{22}, t_{23}\}$ program goes to the next stage of the TLEDA. At this moment, EL.x and EH.x determine low and high threshold for weak pixels to be accepted (x values: 36, 70). After firing of the set $\{t_{24}, t_{25}, t_{26}\}$ the model reached death node.

## 5. EKSPERIMENTAL RESULTS

After careful analisys, the UPN models are transformed into the Python programs.

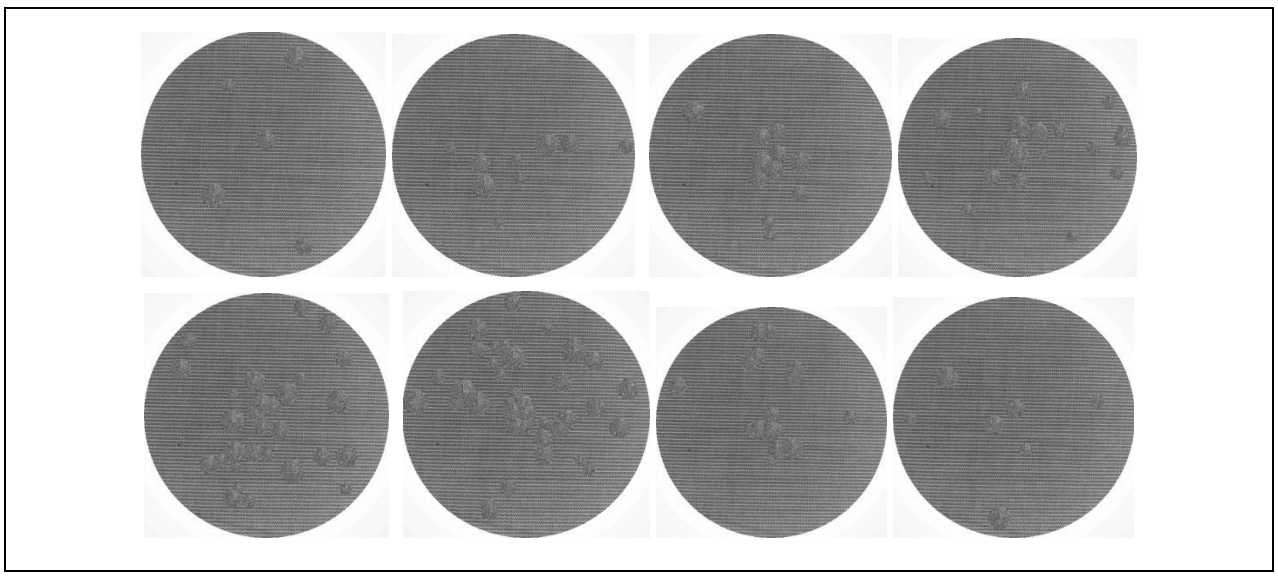

**Figure 4:** Generated images with pilling

One hundred pilling images were generated and then the corresponding images were calculated and created with block comparison and a two-level algorithm edge detection.

Several generated images with pilling are shown at figure 4.

Figure 5. shows the images obtained by the block comparison process.

Figure 6. shows the images representing the output of a two-level edge detection algorithm.

Figure 7. shows image pilling detection speed with respect to comparison block.

Figure 8. shows a diagram of errors that occur during pilling detection depending on the applied block comparison.

The images have generated in order with random pilling (mostly growing).

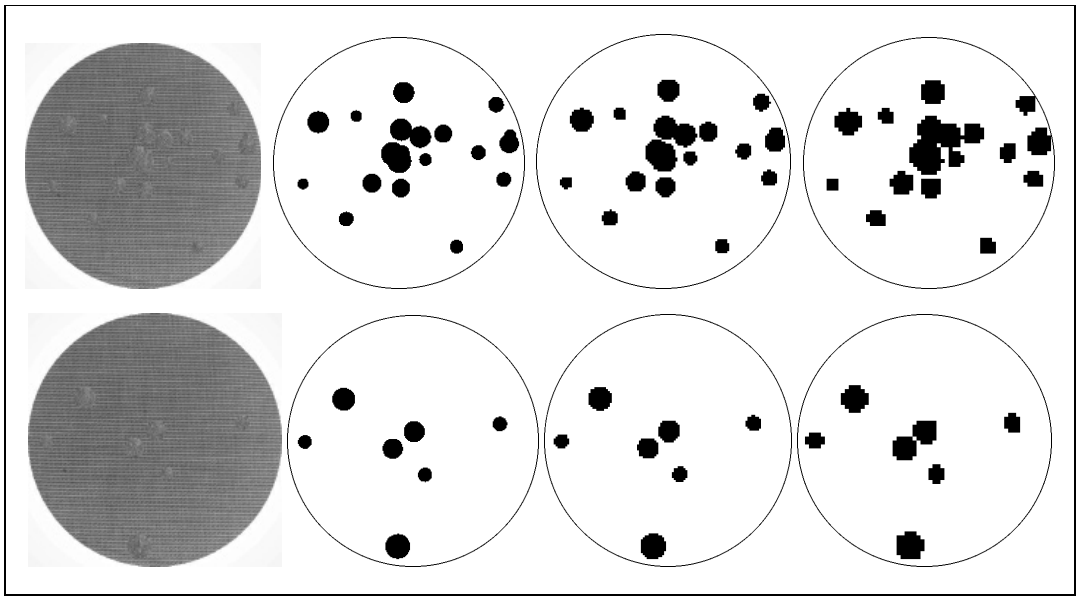

**Figure 5:** Images after block (2x2, 4x4, 8x8) comparison

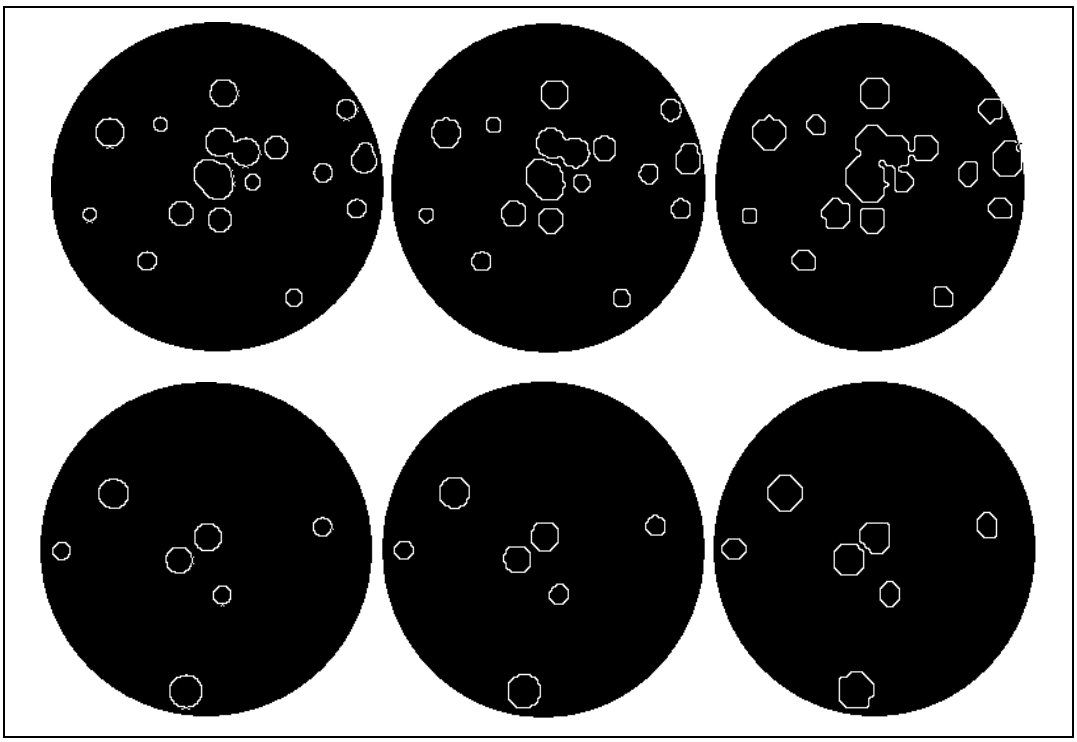

**Figure 6:** Two-level edge detection algorithm output images

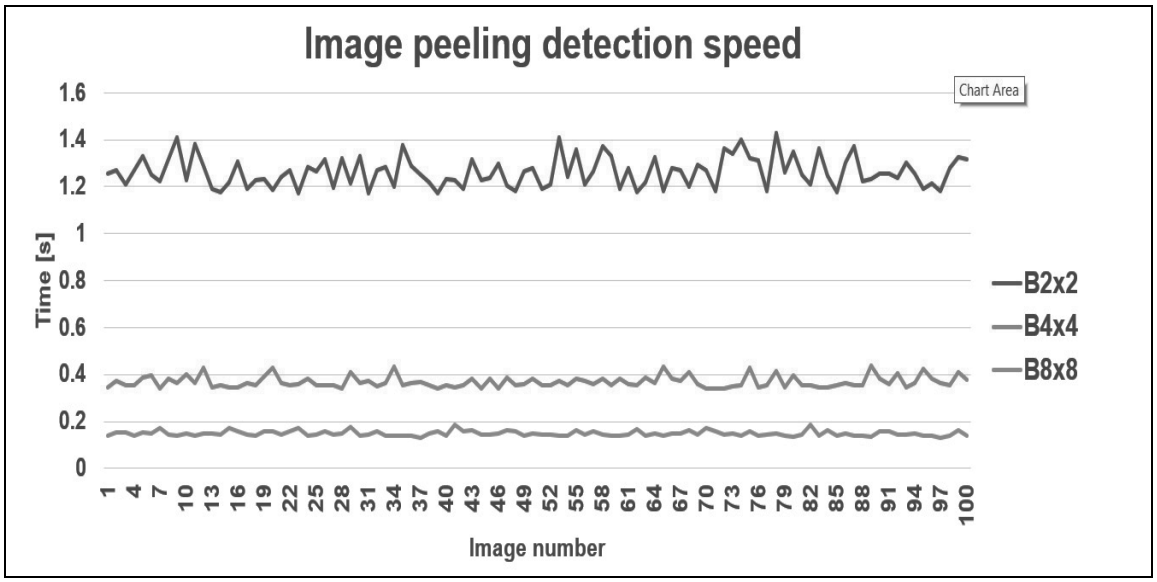


**Figure 7:** Image pilling detection speed

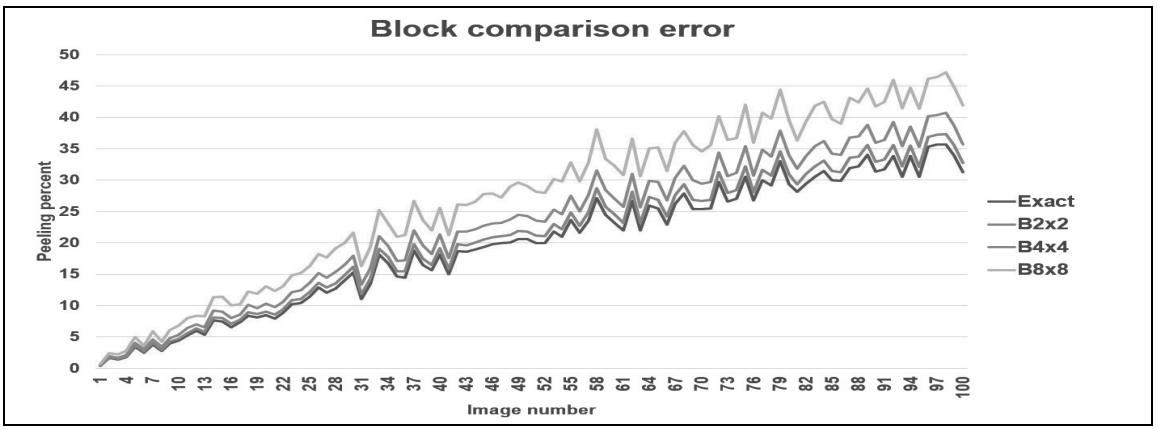


**Figure 8:** Block comparison error

## 6. CONSLUSION

The paper presents a cycle of modeling, simulation, and analysis of the generation and detection of pilling on textiles. The UPN models for generating and detecting pilling have created. These models transformed into Python programs. One hundred images with pilling have generated. An image with pilling was compared with appropriate image without pilling. We used pixel comparison blocks. The prepared images have used as input to a two-level edge detection algorithm. We have shown the diagrams of pilling detection errors and of speed of generating images with detected pilling.

Further research using upgraded Petri nets and a two-level algorithm would be directed towards modeling, simulation, analysis, and detection of water permeability.

## ACKNOWLEDGEMENT

This research was in part supported by the CiS Institute, Belgrade.

## REFERENCES

[1] Radivojević, D., Đorđević, M., Trajković, D. (2016). *Ispitivanje tekstila,* udžbenik Visoka strukovna škola za tekstil u Leskovcu, ISBN 978-86-81087-32-9, Leskovac

[2] Asanović, A., Mihailović T., Nikolić, I., Cerović, D., Mihajlidi, T. (2011). Komparativno ispitivanje otpornosti tkanina prema abraziji, *Tekstilna industrija,* 59 (3), 20-26.

[3] Đorđević, S., Antić, S., Đorđević, D. (2018). Deformacije na istezanje i habanje pamučnih tkanina različitih prepletaja, *Tekstilna industrija* 66 (1), 16-22.

[4] Jankoska, M., Demboski, G. (2017). Uticaj strukture tkanine i finalne obrade na otpornost na cepanje i abraziju, *Tekstilna industrija,* 65 (3), 42-48.

[5] ISO 12945-4 (2010). Textiles- Determination of fabric propensity to surface pilling, fuzzing or matting-Part 4: Assessment of pilling, fuzzing and matting by visual analysis

[6] Radmanovac, N., Ćirković N., Šarac T. (2017). Značaj otpornosti prema habanju u izboru tkanine za zaštitne odevne predmete, *Advanced Technologies,* 6 (1), 81-87.

[7] Tsan-Ming Choi, Information Systems for the Fashion and Apparel Industry, *The Textile Institute and Woodhead Publishing, Woodhead Publishing Series in Textiles*: Number 179.

[8] Štrbac, P. (2002). An approach to modeling communication protocol by using upgraded Petri nets, Ph.D. Dissertation, Military Academy, Belgrade, Serbia.

[9] Štrbac, P., Milovanović G. (2013). Upgraded Petri net model and analysis of adaptive and static arithmetic coding, *Elsevier: Mathematical and Computer Modelling Vol. 58, pp. 1548–1562*.

[10] Canny, J. (1986). A Computational Approach to Edge Detection, *IEEE Transactions on Pattern Analysis and Machine Intelligence, vol. PAMI-8, no. 6*, pp. 679-698.

[11] Štrbac, P., Korać, V., Pejanović, M. (2020). Primena dvonivovskog algoritma za detekciju ivica modelovanog u Nadgrađenoj Petri-mreži, *ETRAN*, *Beograd*, str. 660-666.

Primljeno/Received on: 07.04.2022.

Revidirano/ Revised on: 05.05.2022.

Prihvaćeno/Accepted on: 07.05.2022.